Backbone NMR chemical shift assignment of transthyretin

Bokyung Kim and Jin Hae Kim*

Department of New Biology, Daegu Gyeongbuk Institute of Science and Technology, Daegu 42988, Republic of Korea

Abstract Transthyretin (TTR) is an important transporter protein for thyroxine (T_4) and a holo-retinol protein in human. In its native state, TTR forms a tetrameric complex to construct the hydrophobic binding pocket for T_4. On the other hand, this protein is also infamous for its amyloidogenic propensity, which causes various human diseases, such as senile systemic amyloidosis and familial amyloid polyneuropathy/cardiomyopathy. In this work, to investigate various structural features of TTR with solution-state nuclear magnetic resonance (NMR) spectroscopy, we conducted backbone NMR signal assignments. Except the N-terminal two residues and prolines, backbone ^1H-^{15}N signals of all residues were successfully assigned with additional chemical shift information of ^{13}CO, $^{13}C_\alpha$, and $^{13}C_\beta$ for most residues. The chemical shift information reported here will become an important basis for subsequent structural and functional studies of TTR.

Keywords transthyretin, transthyretin amyloidosis, NMR spectroscopy, chemical shift assignment

Introduction

Transthyretin (TTR) is one of the abundant proteins found in human plasma and cerebrospinal fluid (CSF). The initial name of this protein was prealbumin, as its band in the electrophoresis analysis ran faster than albumin.[1] After identifying its function as a TRANSporter of THYRoxine (T_4; a thyroid hormone) and a holo-RETINol binding protein, it was referred to its current name. In its native state, TTR maintains a β-strand-rich homo-tetrameric complex (~55 kDa), and one of two inter-subunit interfaces in the complex constitutes the hydrophobic binding site for T_4.[2]

In addition to its physiological importance, TTR is well known for its amyloid-forming propensity.[3] TTR is closely correlated with several systemic amyloidosis diseases, e.g., senile systemic amyloidosis (SSA) and familial amyloid polyneuropathy/cardiomyopathy (FAP/FAC). SSA is known to be caused by spontaneous aggregation of wild-type (WT) TTR,[4] while the TTR mutation, which facilitates its aggregation, is the main culprit for FAP and FAC.[5] More than 100 mutations have been reported, and most of these TTR variants exhibits higher aggregation-prone features than the WT protein.[6]

In order to understand physiological and pathological features of TTR, extensive studies using X-ray crystallography has conducted, which contributed much to reveal critical structural characteristics.[7] However, many of the currently available X-ray models are highly similar possibly due to the non-native crystallization condition and crystal packing artifacts, and failed to provide detailed information for dynamic features of TTR. Rather, solution nuclear magnetic resonance (NMR) spectroscopic studies were successful to investigate structural dynamics of TTR; e.g., structural heterogeneity of TTR tetramers,[8] and dynamic feature of TTR monomers.[9–11]

* Address correspondence to: **Jin Hae Kim,** Department of New Biology, Daegu Gyeongbuk Institute of Science & Technology, Daegu 42988, Republic of Korea, Tel: 82-53-785-1770; E-mail: jinhaekim@dgist.ac.kr
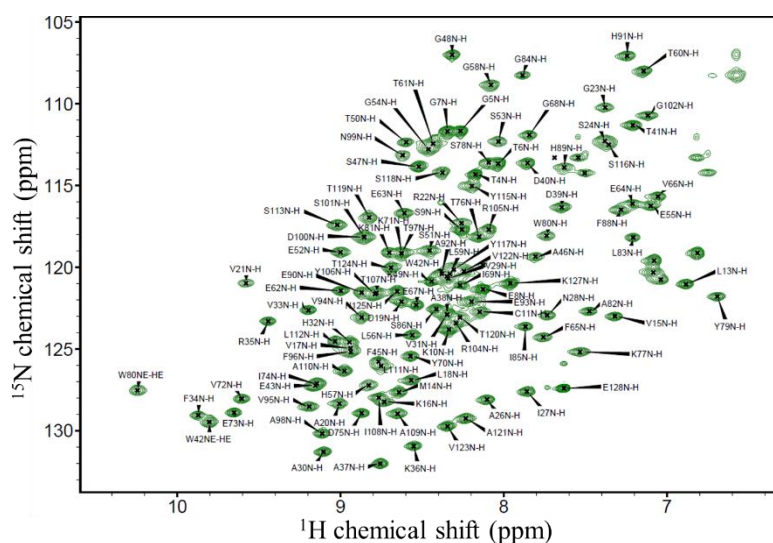
Figure 1. The NMR signal assignment results of TTR noted on its ^{1}H-^{15}N TROSY-HSQC spectrum. Some of the signals at around the chemical shift of 7 ppm were not assigned as they were originated from the side chain of Asn, Gln, Arg, and Lys residues.

We report here the backbone NMR signal assignment results of WT TTR in its tetrameric state. We expect that this result becomes a basis for subsequent structural studies of TTR, as well as for its functional and pathological investigations.

Experimental procedures

For backbone NMR signal assignment of TTR, we employed partial deuteration protocol for better spectral quality of this relatively large homo-tetrameric complex (~55 kDa).[12] The TTR expression plasmid was a generous gift from the group of Markus Zweckstetter.[10] The transformed *E. coli* cells were first inoculated into 3 mL LB media. After overnight incubation at 37 °C, 10 μL from the incubated LB media was transferred to 3 mL M9 media prepared in D$_2$O. After another overnight incubation at 37 °C, 10 μL from the incubated M9 media was transferred to 100 mL M9 media in D$_2$O. The cells were grown overnight at 37 °C, and subsequently transferred to 1 L M9 media in D$_2$O supplemented with ^{15}NH$_4$Cl (0.5 g/L) and [U-^{13}C]-glucose (3 g/L). For expression induction, 0.4 mM IPTG was added when OD$_{600}$ reached at 0.4, after which cells were further grown

overnight. The final cells were harvested with centrifugation at 4000 g for 20 min, and the resultant pellets were stored at -80 °C until used. Purification of TTR was conducted as reported previously.[10,11]

NMR data was acquired with a 600-MHz NMR spectrometer (Bruker) equipped with a cryogenic HCN probe. The sample for backbone signal assignment was prepared as 0.5~1 mM of partially deuterated [U-^{13}C;U-^{15}N]-TTR along with the buffer of 50 mM MES pH 6.5, 100 mM NaCl, 5 mM dithiothreitol, 0.01% NaN$_3$, and 7% D$_2$O. The following NMR spectra was obtained: 2D ^{1}H-^{15}N TROSY-HSQC, 3D TROSY-HNCO, 3D TROSY-HNCA, 3D TROSY-HN(CO)CA, and 3D TROSY-HNCACB. The raw data was processed with TopSpin (Bruker), and subsequently analyzed with NMRFAM-Sparky.[13]

Results and discussion

The partial deuteration protocol successfully enhanced spectral quality of WT TTR, enabling us to obtain the partially deuterated [U-^{13}C;U-^{15}N]-TTR sample in a sufficient yield (~10 mg/L) and to complete the backbone signal assignment. Due to the relatively

large size of the tetrameric complex, transverse relaxation-optimized spectroscopy (TROSY) was employed to obtain high signal-to-noise ratio spectra. For backbone assignment procedure, we collected 2D ^{1}H-^{15}N TROSY-HSQC, 3D TROSY-HNCO, 3D TROSY-HNCA, 3D TROSY-HN(CO)CA, and 3D TROSY-HNCACB spectra, all of which were analyzed together for complete backbone assignment. The signal assignment result marked on the ^{1}H-^{15}N TROSY-HSQC spectrum is shown in Fig. 1, and the entire chemical data is tabulated in Table 1. Except the N-terminal two residues and prolines, the ^{1}H-^{15}N signals from all the residues were successfully assigned, and there was no signal left unassigned in the ^{1}H-^{15}N TROSY-HSQC spectrum with the exception for the signals originating from the sidechain ^{1}H-^{15}N pairs.

As we were able to have almost complete signal

Table 1. The backbone signal assignment results of TTR.

Residue	^{13}CO	^{13}C$_\alpha$	^{13}C$_\beta$	^{1}H$_N$	^{15}N$_H$	Residue	^{13}CO	^{13}C$_\alpha$	^{13}C$_\beta$	^{1}H$_N$	^{15}N$_H$	Residue	^{13}CO	^{13}C$_\alpha$	^{13}C$_\beta$	^{1}H$_N$	^{15}N$_H$
P3	174.8	65.2	33.5	-	-	F45	170.9	61.1	44.5	8.8	125.7	P87	172.4	63.4	35.6	-	-
T4	172.6	63.9	71.5	8.2	114.3	A46	172.5	54.3	24.8	7.8	119.3	F88	173.2	62.3	42.6	7.3	116.5
G5	171.9	47.3	-	8.3	111.6	S47	169.9	59.8	67.7	8.5	113.8	H89	175.1	60.1	33.2	7.6	113.9
T6	172.7	63.9	71.5	8.0	113.6	G48	168.2	47.7	-	8.3	106.9	E90	172.7	60.1	32.7	8.9	121.5
G7	171.6	47.3	-	8.3	111.6	K49	173.5	55.7	37.5	8.4	120.9	H91	170.2	56.6	32.2	7.2	107.0
E8	174.1	58.4	31.8	8.1	121.3	T50	173.1	64.2	71.9	8.6	112.3	A92	172.7	53.8	21.4	8.4	120.4
S9	172.1	60.4	65.5	8.3	117.7	S51	172.9	59.2	67.5	8.5	119.0	E93	172.2	56.4	34.5	8.2	122.1
K10	173.1	57.6	34.3	8.3	123.8	E52	173.1	61.0	30.4	9.0	119.1	V94	172.2	63.4	36.6	8.9	123.0
C11	-	-	29.5	8.1	122.6	S53	173.3	59.7	65.9	8.0	112.3	V95	172.8	63.1	35.6	9.2	128.5
P12	170.6	66.2	34.5	-	-	G54	169.7	47.4	-	8.5	112.8	F96	169.1	58.0	-	8.9	125.1
L13	170.3	55.7	45.8	6.9	121.0	E55	173.3	56.4	34.5	7.1	116.2	T97	170.8	64.9	70.7	8.6	119.1
M14	171.1	56.8	36.9	8.6	127.6	L56	172.2	56.1	45.2	8.6	124.1	A98	174.0	52.0	25.4	9.1	130.1
V15	170.5	62.0	36.6	7.3	123.0	H57	172.7	57.6	-	8.8	127.0	N99	172.5	56.3	39.0	8.6	113.1
K16	-	56.5	37.5	8.7	128.2	G58	172.9	48.6	-	8.1	108.8	D100	174.7	57.4	41.9	8.9	118.1
V17	171.4	62.6	34.6	8.9	124.9	L59	173.4	59.3	44.9	8.3	120.4	S101	171.5	59.2	65.4	8.9	118.2
L18	171.3	55.7	47.7	8.6	126.9	T60	170.0	61.4	69.9	7.1	108.0	G102	-	45.5	-	7.1	110.7
D19	174.2	55.2	43.6	8.6	122.1	T61	172.6	61.5	74.2	8.4	112.4	P103	175.4	65.6	33.4	-	-
A20	174.6	55.6	21.0	9.0	128.1	E62	175.6	62.0	31.4	9.0	121.4	R104	171.3	55.3	35.2	8.3	123.4
V21	-	67.4	32.9	9.6	120.9	E63	175.4	61.2	30.9	8.6	116.7	R105	172.4	56.6	32.5	8.1	117.7
R22	174.3	57.2	-	8.3	117.3	E64	174.3	59.0	32.8	7.2	116.1	Y106	172.9	59.8	43.4	8.8	121.7
G23	170.7	49.2	-	7.4	110.2	F65	171.1	57.0	39.1	7.8	124.3	T107	170.6	63.9	71.8	8.8	121.5
S24	-	57.2	68.7	7.4	112.2	V66	174.4	62.1	34.7	7.1	115.7	I108	170.3	60.4	39.8	8.8	128.0
P25	172.2	64.8	32.8	-	-	E67	173.4	58.8	30.9	8.5	122.3	A109	174.7	51.2	22.4	8.6	128.9
A26	172.3	52.6	19.6	8.1	128.1	G68	167.1	46.7	-	7.8	111.8	A110	171.2	52.3	22.9	9.0	126.3
I27	172.2	63.8	40.9	7.9	127.6	I69	171.5	62.8	39.7	8.3	121.1	L111	173.4	55.8	45.5	8.7	126.0
N28	172.2	56.5	38.9	7.7	122.9	Y70	170.7	58.4	43.6	8.6	125.4	L112	173.2	57.6	45.8	9.0	124.6
V29	173.5	63.7	32.9	8.3	120.7	K71	172.4	55.5	37.0	8.6	119.2	S113	-	-	-	9.0	117.4
A30	173.5	54.7	21.2	9.1	131.3	V72	171.3	63.1	34.6	9.6	128.0	P114	-	68.8	-	-	-
V31	171.5	62.5	35.9	8.3	122.8	E73	172.3	57.2	34.0	9.6	128.9	Y115	170.8	60.3	-	8.2	115.0
H32	170.0	57.0	-	8.9	124.5	I74	173.8	62.3	41.3	9.1	127.1	S116	169.7	59.3	67.7	7.4	112.4
V33	172.6	61.9	34.3	9.2	122.6	D75	173.8	55.3	40.2	8.9	128.9	Y117	170.5	59.2	43.3	8.3	120.1
F34	170.6	58.2	46.2	9.9	129.0	T76	172.5	66.4	67.8	8.1	118.1	S118	171.1	57.3	67.7	8.4	114.2
R35	172.5	56.3	35.5	9.4	123.3	K77	176.3	62.3	34.4	7.5	125.2	T119	-	60.6	73.1	8.8	116.9
K36	173.2	59.2	33.4	8.6	130.9	S78	174.0	63.8	-	8.1	113.6	T120	169.5	63.1	73.5	8.3	123.1
A37	175.8	52.9	22.1	8.8	132.0	Y79	173.9	63.1	39.2	6.7	121.8	A121	171.7	51.7	22.2	8.2	129.3
A38	174.9	56.1	19.9	8.3	122.9	W80	177.5	61.3	31.0	7.7	118.0	V122	173.0	62.5	35.0	8.2	120.2
D39	173.2	55.2	41.2	7.6	116.3	K81	178.8	61.5	32.9	8.7	119.1	V123	173.4	63.1	35.0	8.3	129.7
D40	172.3	58.2	40.9	7.9	113.6	A82	176.2	56.4	19.3	7.5	122.7	T124	170.2	62.2	73.1	8.7	120.0
T41	170.2	63.5	72.6	7.2	111.3	L83	174.7	56.4	43.9	7.2	118.2	N125	-	52.4	40.4	8.7	121.5
W42	172.9	57.6	32.0	8.4	120.6	G84	171.4	47.5	-	7.9	108.2	P126	173.6	65.4	-	-	-
E43	-	55.1	32.9	9.2	127.3	I85	171.7	61.6	42.4	7.9	123.6	K127	172.8	58.0	34.1	8.0	121.0
P44	172.9	66.8	33.3	-	-	S86	-	56.8	64.8	8.4	122.5	E128	-	59.9	32.5	7.6	127.4

assignment results, we expect that our data provide a solid basis for subsequent NMR-based structural studies. Based on this result, we are currently conducting several subsequent studies to reveal heterogeneous structural states of TTR in various conditions, with which we hope to contribute to appreciate diverse physiological and pathological features of TTR.

Acknowledgements

References

1. S. H. Ingbar, *Endocrinology* **63**, 256 (1958)
2. C. C. F. Blake, M. J. Geisow, S. J. Oatley, B. Rérat, and C. Rérat, *J. Mol. Biol.* **121**, 339 (1978)
3. B. Kim and J. Kim, *J. Kor. Magn. Reson. Soc.* **24**, 91 (2020)
4. P. Westermark, K. Sletten, B. Johansson, and G. G. Cornwell, *Proc. Natl. Acad. Sci. U. S. A.* **87**, 2843 (1990)
5. P. P. Costa, A. S. Figueira, and F. R. Bravo, *Proc. Natl. Acad. Sci. U. S. A.* **75**, 4499 (1978)
6. L. H. Connors, A. Lim, T. Prokaeva, V. A. Roskens, and C. E. Costello, *Amyloid* **10**, 160 (2003)
7. S. K. Palaninathan, *Curr. Med. Chem.* **19**, 2324 (2012)
8. J. K. Das, S. S. Mall, A. Bej, and S. Mukherjee, *Angew. Chemie - Int. Ed.* **53**, 12781 (2014)
9. K. H. Lim, H. J. Dyson, J. W. Kelly, and P. E. Wright, *J. Mol. Biol.* **425**, 977 (2013)
10. J. Kim, J. Oroz, and M. Zweckstetter, *Angew. Chemie - Int. Ed.* **55**, 16168 (2016)
11. J. Oroz, J. Kim, B. J. Chang, and M. Zweckstetter, *Nat. Struct. Mol. Biol.* **24**, 407 (2017)
12. J. T. Hoopes, M. A. Elberson, R. J. Preston, P. T. Reddy, and Z. Kelman, *Method. Enzymol.* **565**, 27 (2015)
13. W. Lee, M. Tonelli, and J. L. Markley, *Bioinformatics* **31**, 1325 (2015)